E.92. Abou Tabl

DIVIDED-WINDING-ROTOR SYNCHRONOUS GENERATOR ANALYTICAL STUDY OF THE NO-LOAD FIELD DISTRIBUTION

BY

Dr. Ing. Hassan Ali Abou-Tabl, B.Sc., Ph.D.*

ABSTRACT:

This paper presents an analytical study of the resultant m.m.f. distributions in the air-gap of a divided-winding-rotor synchronous generator. For linear analysis, the principle of superpostion can be applied to obtain these distributions graphically. The study makes use of the no-load field control factors to obtain the actual per-unit maximum values of both field components while the resultant field is shifted in steps w.r.t. the rotor. The obtained waveforms exhibits the possibility of summarising them in a group of representative waveforms which enable us to study the effect of shift-angle, as well as the pole winding spread, on the resultant m.m.f. The m.m.f. distributions obtained experimentaly, are compared with those analytically obtained. The results show that they are in good agreement. The conditions required to simulate the coventional field distribution by a divided-winding - rotor are stated and discussed.

0. Nomenclature:

F_c : = coventional m.m.f. distribution, sinusoidal peak;

$(F_c)_{max}$: = maximum conventional m.m.f. distribution, nonsinusoidal;

F_{cn} : = the nth harmonic peak of a conventional m.m.f. distribution;

F_R : = resultant m.m.f. distribution, sinusoidal peak;

F_a : = active-component of F_R, sinusoidal peak;

F_r : = reactive-component of F_R, sincusoidal peak;

$(F_R)_{max}$: = maximum resultant m.m.f. distribution, nonsinusoidal;

$(F_a)_{max}$: = maximum active-component of $(F_R)_{max}$, nonsinusoidal;

$(F_r)_{max}$: = maximum reactive-component of $(F_R)_{max}$, nonsinusoidal;

h_n : = the nth harmonic peak ratio;

$(I_f)_c$: = conventional excitation current;

$(I_f)_a$: = active-excitation current, peak, sinusoidal distribution;

$(I_f)_r$: = reactive-excitation current, peak, sinusoidal distribution;

---

* Lecturer, Faculty of Engineering, El-Mansoura University. El-Mansoura, Egypt.

Mansoura Bulletin, June 1979.

$(I_f)_{d.w.}$: = no-load excitation current in either axis alone to get rated no-load voltage, peak, sinusoidal distribution;

$(\bar{I}_f)_a$, $(\bar{I}_f)_r$, and $(\bar{I}_f)_{d.w.}$: defined as above but for rectangular distribution, same but lower case letters refer to per-unit values;

$(N_f)_c$: = number of turns per pole of a c.w.r.;

$(N_f)_{d.w.}$: = number of turns per half-pole in either the active or reactive-field winding;

n : = harmonic order;

θ' : = shift-angle, measured from the 180°-active axis;

τ : = pole-winding-spread;

2β : = pole-arc $= \pi - \tau$;

α : = $\beta/2$;

c.w.r. : = conventional-winding-rotor;

d.w.r. : = divided-winding-rotor;

1. INTRODUCTION:

In a previous work[1] the no-load field control factors, C_a and C_r, were introduced to adjust the no-load excitation of a d.w.r. synchronous generator. The derivation of these factors assumes a sinusoidal no-load field distribution of each of the resultant field F_R as well as of its components F_a and F_r. Accordingly, the resultant field can be held constant when it is shifted around the rotor by introducing the proper excitation currents $(I_f)_a$ and $(I_f)_r$ in the corresponding field winding. Both currents are also assumed to have sinusoidal distributions around the rotor.

This assumption is not valid in an actual d.w.r. where rectangular field-current distributions take place. Actually, it is not expected to obtain sinusoidal field distributions due to such field-current distributions.

Experimental investigations were carried out on a machine model to simulate the no-load field distribution curves of a d.w.r. at different shift-angle θ'. Excitation currents $(\bar{I}_f)_a$ and $(\bar{I}_f)_r$ were adjusted to correspond to their maximum fundamental values. The oscillographs obtained gave the impression that the no-load m.m.f. wave-shape is greatly affected by the pole-winding-spread τ and the shift-angle θ'.

This paper presents an analytical study of the resultant no-load m.m.f. waveforms of a d.w.r. The study aims to have a theoretical approach of the effect of shift-angle, as well as the pole-winding-spread, on the actual m.m.f. distribution.

For the purpose of comparison, a brief account on the no-load m.m.f. distribution established in the air gap of a c.w.r. synchronous generator is presented first.

2. Conventional-Winding-Rotor, M.M.F. Distribution

Considering a 2-pole cylindrical rotor, the actual m.m.f. distribution in air gap has a stepped waveform which differs in shape according to the pole-winding-spread τ. For purpose of machine analysis the stepped m.m.f. waveform is replaced by an equivalent triangular or trapezoidal m.m.f. waveform for $\tau \leq 180^{\circ}$ respectively. These smoothed waveforms, Fig. 1, are established by the uniform distributed excitation current (neglecting rotor slotting).

The derivation of the e.m.f. equation of a c.w.r. synchronous generator depends essentialy on the assumption of sinusoidally distributed no-load m.m.f.[2,3]. Accordingly, the equivalent m.m.f. waveform must approximate the sinusoidal shape. This can best be judged by the Fourier-Series of the actual (equivalent) m.m.f. waveforms.

2.1. Harmonic Content of Conventional Field Distribution:

All three m.m.f. distributions, Fig. 1, of a conventional winding-rotor are true alternating waves and ensure the symmetry conditions[4]:

$$F_c(x) = -F_c(x + \pi) \qquad \ldots\ldots(1.1)$$

and

$$F_c(\pi/2 - x) = F_c(\pi/2 + x), \qquad \ldots\ldots(1.2)$$

where x is the angular displacement, in electrical radiances, measured from a point at which $F_c(x) = 0$. The Fourier-Series of such a type of wave contains odd harmonics only of sine terms, thus

$$F_c(x) = \sum_{n=1}^{n=\infty} F_{cn} \operatorname{Sin}(nx) \qquad \ldots\ldots(2)$$

In this relation F_{cn} is the peak of the nth harmonic which can be given by:

$$F_{cn} = \frac{4}{\pi} \int_0^{\pi/2} F_c(x) \sin(nx)\, dx.$$

From this integration, the nth harmonic peak ratio of a given m.m.f. waveform can be obtained as:

$$h_n = F_{cn} / (F_c)_{max} \qquad \ldots\ldots(3)$$

$$= (4/\pi n^2)(2/\tau) \operatorname{Sin}(n\tau/2) \qquad \ldots\ldots(4)$$

This relation is calculated for three different pole-winding-spreads to explain their effect on the harmonic content of a conventional field distribution. Results are listed in Table (1).

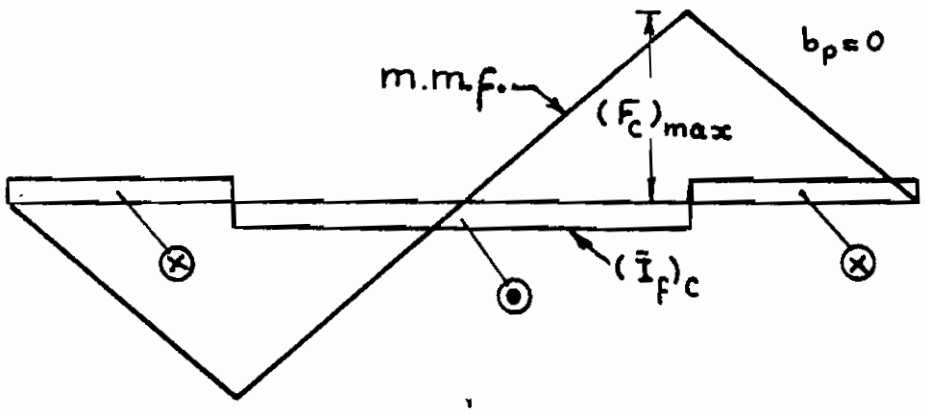

(a) 180° - pole winding spread

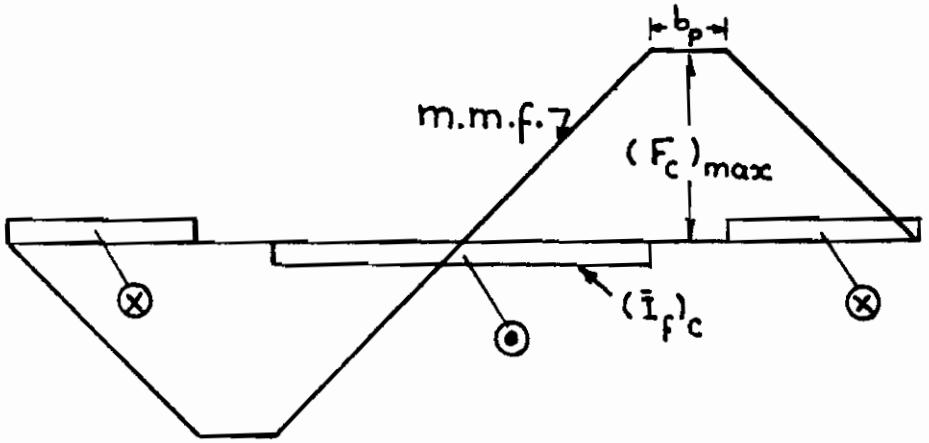

(b) 150° - pole winding spread

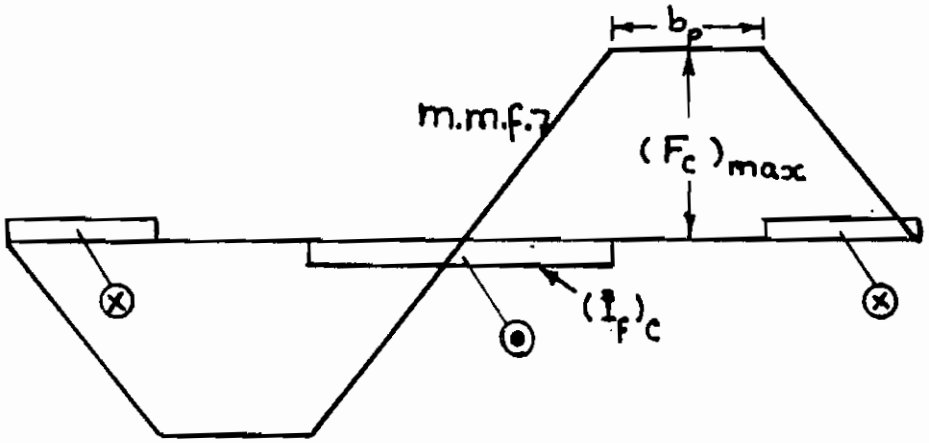

(c) 120° - pole winding spread

Fig. 1 : M.M.F. Distribution Curves of 2-pole C.W.R.

2.2. Choice of the Pole-Winding-Spread:

Assuming that the air gap reluctance is constant (uniform air gap) and neglecting the saturation, the flux density curve comes similar in shape to that of the m.m.f. waveform. Therefore the ratio (a_1/a) of either the m.m.f. or the flux-density distribution is the same;

$$(a_1/a) = \frac{\text{Fundamental half-wave area}}{\text{Actual half-wave area}} \quad \ldots\ldots(5)$$

This ratio indicates how much is the sinusoidal flux per pole compared with the actual flux per pole, Table (1).

If both ratios, h_1 and (a_1/a), are close in value to unity then it can be assumed that the flux per pole is invariable when the actual flux density curve is replaced by its fundamental. Higher harmonics can be neglected or taken into account by having their peaks within very small limits[3]. This can be ensured by the optimum choice of the pole-winding-spread as well as the type of armature winding.

Table (1)

Pole-winding -spread τ	Harmonic Peak Ratios					(a_1/a)
	F_{c1}	F_{c3}	F_{c5}	F_{c7}	F_{c9}	
180°	0.811	0.090	0.032	0.017	0.010	1.033
150°	0.940	0.076	0.010	0.005	0.008	1.026
120°	1.053	0.000	0.042	0.021	0.000	1.006

It is evident from Table (1) that the pole-winding-spread τ has a considerable effect on the harmonic content of the corresponding field distribution. A pole-winding-spread of 120° seems to be the best choice for the following reasons:

1) the fundamental peak ratio (h_1) is about unity;
2) the tripple harmonics are abscent; and
3) the ratio (a_1/a) is close to unity.

Further, this pole-winding-spread is often chosed by designers because it allows enough place to accumulate the damper winding.

It can be concluded that the approximation of the actual m.m.f. distribution of more realistic c.w.r. by its fundamental is accurate enough for the purpose of machine-analysis.

3. Divided-Winding-Rotor, M.M.F. Distribution:

The two separate field windings on the d.w.r., are considered to costitute the same number of half-poles. Either field winding has its own m.m°f. distribution which is shifted from

the other by an angle equal to $\tau/2$. For linear analysis, the resultant no-load m.m.f. in the air gap can be obtained graphically by applying the principle of superposition to the two distributions[5] mentioned above. The method of obtaining the no-load resultant m.m.f. distribution of a d.w.r., in accordance with a given shiftangle, will be discussed in following.

3.1. Per-Unit Excitation Currents:

The excitation currents $(I_f)_a$ and $(I_f)_r$, represent the maximum sinusoidal values[1] required in accordance with a given shift-angle θ'. They are expressed as

$$(I_f)_a = C_a\ (I_f)_{d.w.} \qquad \ldots\ldots(6.1)$$

$$(I_f)_r = C_r\ (I_f)_{d.w.} \qquad \ldots\ldots(6.2)$$

where C_a and C_r are the no-load field control factors;

$$C_a = \mathrm{Cos}(\theta' + \alpha)/\ \mathrm{Cos}\ 2\alpha \qquad \ldots\ldots(7.1)$$

and

$$C_r = \mathrm{Sin}(\theta' - \alpha)/\ \mathrm{Cos}\ 2\alpha\ . \qquad \ldots\ldots(7.2)$$

$(I_f)_{d.w.}$ is the maximum sinusoidal excitation current required in either field winding, acting alone to induce the rated sinusoidal no-load voltage.

A sinusoidal distribution of both currents is not possible in an actual divided-winding-rotor. Fig. 2 gives a developed form of a 2-pole d.w.r. for the three different pole-winding-spread: 180°, 150°, and 120°. Current sheets (a, a') and (r, r') represent the active-and reactive-excitations respectively. It is assumed that both excitation currents are uniformly distributed in form of a rectangular wave.

Sinusoidally distributed excitation currents can be assumed as the fundamentals of the corresponding rectangular distributions. Therefore actual excitation currents, represented by the hights of the rectangular distributions, can be given in terms of the peaks of their corresponding fundamentals[4]:

$$(\bar{I}_f)_a = (\pi/4)(C_a\ (I_f)_{d.w.}) = C_a(\bar{I}_f)_{d.w.} \qquad \ldots\ldots(8.1)$$

and

$$(\bar{I}_f)_r = (\pi/4)(C_r\ (I_f)_{d.w.}) = C_r(\bar{I}_f)_{d.w.} \qquad \ldots\ldots(8.2)$$

where

$$(\bar{I}_f)_{d.w.} = (\pi/4)(I_f)_{d.w.}\ . \qquad \ldots\ldots(9)$$

Referring both currents $(\bar{I}_f)_a$ and $(\bar{I}_f)_r$ to $(\bar{I}_f)_{d.w.}$, the per-unit excitation currents for a given shift-angle can be obtained as

$$(i_f)_a = C_a \qquad \ldots\ldots(10.1)$$

$$(i_f)_r = C_r \qquad \ldots\ldots(10.2)$$

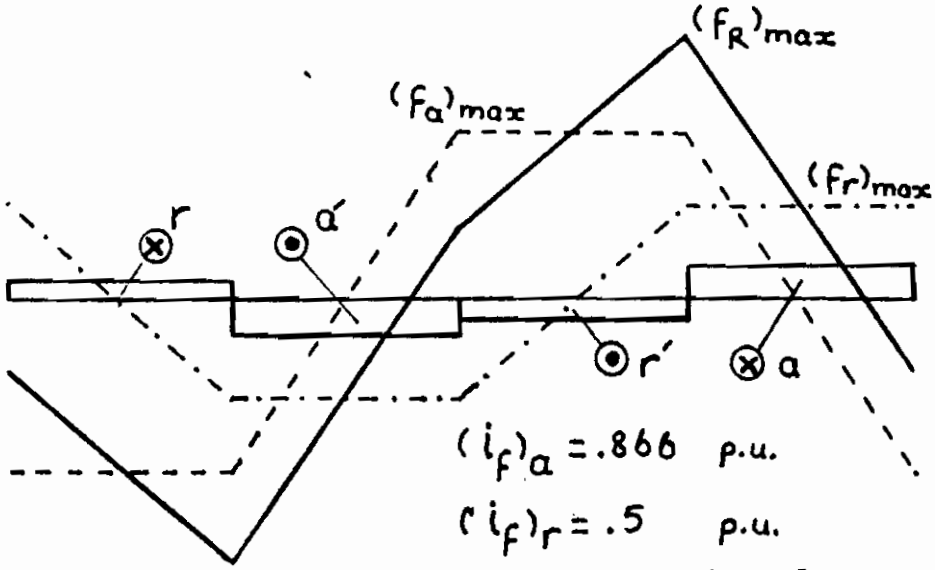

(a) 180°-pole winding spread, $\theta' = 30°$

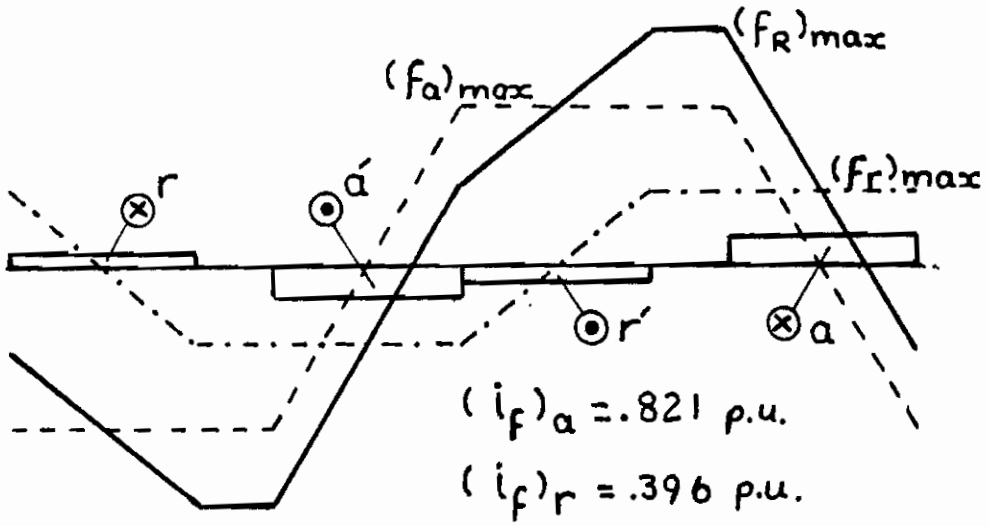

(b) 150°-pole winding spread, $\theta' = 30°$

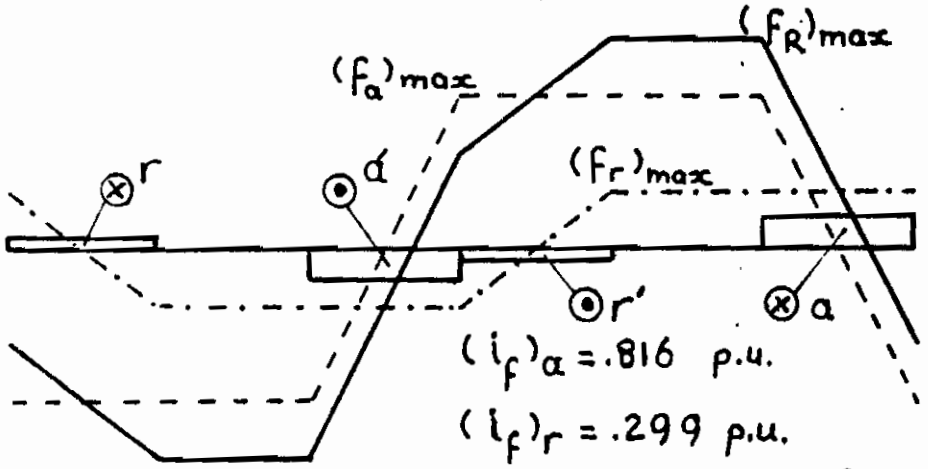

(c) 120°-pole winding spread, $\theta' = 30°$

Fig. 2 : Resultant M.M.F. Distribution of 2-pole D.W.R., (example).

These relations indicate that the p.u. values of excitation currents are numerricaly equal to the corresponding no-load field control factors.

3.2. Per-unit Maximum values of M.M.F. Components:

An actual m.m.f. distribution of either field-winding has an absolute maximum value which is proportional to the corresponding excitation current. For a given shift-angle, both excitation currents have their magnitudes according to equations (8). Assuming that both field windings have the same number of turns, the field component maximum values $(F_a)_{max}$ and $(F_r)_{max}$ are given by

$$(F_a)_{max} = \pm C_a (\bar{I}_f)_{d.w.}(N_f)_{d.w.} \quad \ldots\ldots(11.1)$$

$$(F_r)_{max} = \pm C_r (\bar{I}_f)_{d.w.}(N_f)_{d.w.} \quad \ldots\ldots(11.2)$$

As the value of product $(\bar{I}_f)_{d.w}\,(N_f)_{d.w.}$ is constant, both components will have the same per-unit maximum values as the per-unit excitation currents; i.e.

$$(f_a)_{max} = \pm C_a \quad \ldots\ldots(12.1)$$

$$(f_r)_{max} = \pm C_r \quad \ldots\ldots(12.2)$$

These per-unit maximum values of the m.m.f. components help constructing the corresponding distributions and obtaining the per-unit maximum value of the resultant m.m.f. distribution.

3.3. Resultant M.M.F. Distribution:

Having obtained the per-unit maximum values of the m.m.f. components and the spatial distribution of both excitation currents in developed form, the individual distributions of the active and reactive m.m.fs. can be constructed. While the spatial limits of each m.m.f. distribution towards the rotor circumference are directed by the pole-winding-spread, its absolute maximum value corresponds to the shift-angle as well as to the pole-winding-spread. Distribution polarity is defined by the sign of the corresponding no-load field cotrol factor.

For linear analysis, the actual resultant m.m.f. can be obtained by adding, point by point, the available m.m.f. components. Figure 2 shows the resultant m.m.f. distribution together with its component's distributions, at the same shift-angle ($\theta' = 30$) for the three given pole-winding-spreads. The absolute maximum value of the resultant field is generally given by

$$(F_R)_{max} = \pm((F_a)_{max} + (F_r)_{max})$$

$$= \pm (C_a + C_r)(\bar{I}_f)_{d.w.}(N_f)_{d.w.} \quad \ldots\ldots(13)$$

or in per-unit

$$(f_R)_{max} = \pm (C_a + C_r) \qquad \ldots\ldots(14)$$

The per-unit maximum value of a resultant distribution is equal to the sum of the per-unit maximum values of its components. It is evident that the resultant distributions, Fig. 2, are neither the same in shape nor in their maximum values, $(F_R)_{max}$.

4. Shift-Angle Effect on the Resultant M.M.F. Distribution:

In order to study the effect of the shift-angle on the resultant m.m.f. waveform, the resultant field is shifted in steps around the rotor and the corresponding resultant distribution is obtained. It is found that the resultant waveforms obtained when the value of θ' lies between the active-and direct-axis, are the mirror images to those obtained when the value of θ' lies between the direct-and reactive-axis. The same thing can be said about the resultant m.m.f. distributions obtained for shift - angles about the quadrature-axis. Therefore, the summarised wave-shapes are given in Fig. 3 for θ' laying between the direct- and quadrature-axis as representative examples. It is seen that the resultant field distribution begins on the d-axis and sweeps towards the q-axis with advanced θ'.

For 180°-pole winding spread the m.m.f. waveforms obtained about the d-axis are identical to those obtained about the q-axis. For a pole-winding-spread less than 180°, it is seen from Fig. 3 that they are not identical. Waveforms obtained about the q-axis are so greatly distorted. Not only the wave-shape which is distorted, but also its duration becomes less as a result of this distortion.

Distortion in half-wave duration occurs at a time when the resultant field is along the q-axis. In this case, regions of zero m.m.f. are more wider than a plane. The effective half-wave duration becomes as small as 5/6 a pole-pitch for $\tau = 150°$, and as small as 2/3 a pole-pitch for a $\tau = 120°$. In general, therefore, the efficitive half-wave duration becomes equal to the corresponding pole-winding-spread.

It is also evident from Fig. 3 that the maximum resultant field $(F_R)_{max}$ does not remain constant as the resultant field is shifted. The variation of $(F_R)_{max}$ with θ' illustrates the relative variation in the maximum resultant field. In shifting the resultant field axis away from the d-axis towards the reactive-axis, the magnitude of $(F_R)_{max}$ is decreased. Having the resultant field along the reactive-axis, the resultant distribution is that of the reactive-component acting alone. In this case $(F_R)_{max}$, the hight of a trapezoidal distribution, is equal to one per-unit. Further shifting towards the q-axis causes the value of $(F_R)_{max}$ to increase until it reaches its largest value when the resultant field axis coincides with the q-axis.

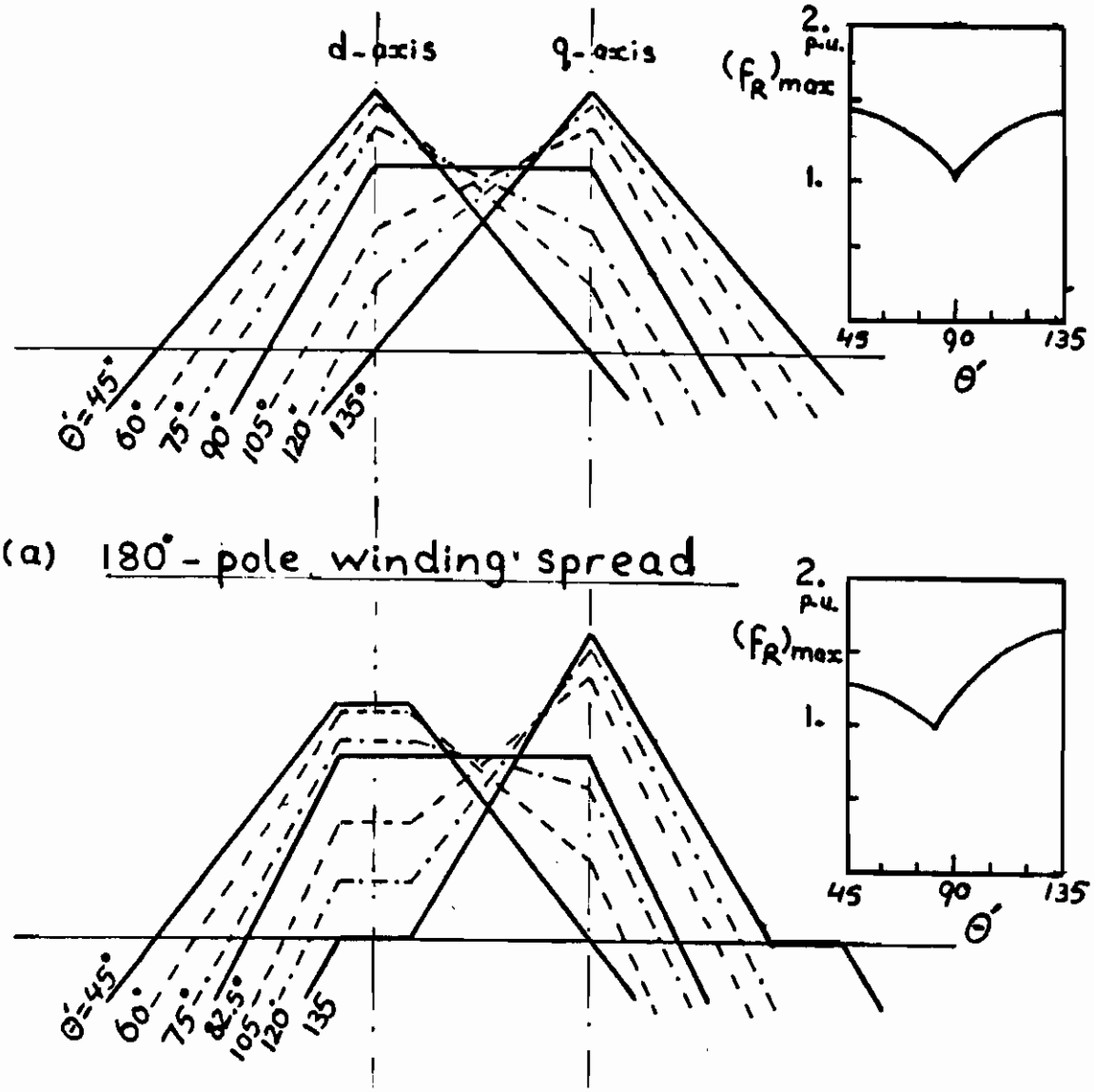

(a) 180°-pole winding spread

(b) 150°-pole winding spread

(c) 120°-pole winding spread

Fig.3 Summarised Groups of Resultant M.M.F. Waveforms of 2-Pole D.W.R.

Comparison of the resultant waveforms obtained analytically with those obtained by experimental model (Fig. 4) shows that these are in agreement. It should be noted that only oscillographs for $\tau = 180°$ and $120°$ are given in Fig. 4. This is due to the limited machine model facilities.

5. Conventional Field Simulation by a D.W.R.:

Comparing the resultant distributions obtained when the resultant field axis is along the d-axis ($\theta' = 45°$) with the corresponding conventional distributions of Fig. 1, it is found that these are the same. In order to simulate the conventional field distribution by a d.w.r. the two following conditions must hold;

1) both the active-and reactive-excitation currents are equal

$$(\bar{I}_f)_a = (\bar{I}_f)_r = C\,(\bar{I}_f)_{d.w.} \qquad \ldots\ldots(15)$$

where $C_a = C_r = C$. This condition results in symmetrical distribution of the resultant field about the pole-axis (d-axis) as it is with the conventional field. Under this condition, the resultant field distribution corresponds to a shift-angle $\theta' = 45°$, and has the same pole-arc as the conventional distribution.

2) each of the active-and reactive-excitation current is equal to the conventional excitation current

$$C(\bar{I}_f)_{d.w.} = (\bar{I}_f)_c \qquad \ldots\ldots(16)$$

This condition results in equal maximum values for both the resultant and conventional distributions. This can be proved by assuming that

$$(N_f)_{d.w.} = (1/2)(N_f)_c,$$

and going back to equation (13) under the assumption of equation (16), then

$$(F_R)_{max,\ 45°} = \pm\,(\bar{I}_f)_c (N_f)_c = (F_c)_{max} \qquad \ldots\ldots(17)$$

If both of these conditions hold then a divided-winding -rotor can be considered as a conventional one. In this case, the no-load m.m.f. distribution established in the air-gap is identical to that established by a c.w.r. The m.m.f. oscillographs obtained from the d.w.r. synchronous generator model, by applying these conditions, are identical to those obtained from the same machine with its rotor connected in conventional form. This is evident when the resultant oscillographs obtained at $\theta' = +5°$ are compared with those marked "conv." in Fig. 4.

6. CONCLUSION:

The study demonstrate an analytical method to obtain the actual m.m.f. distribution at no-load of a d.w.r. synchronous generator in accordance with a given shift-angle.

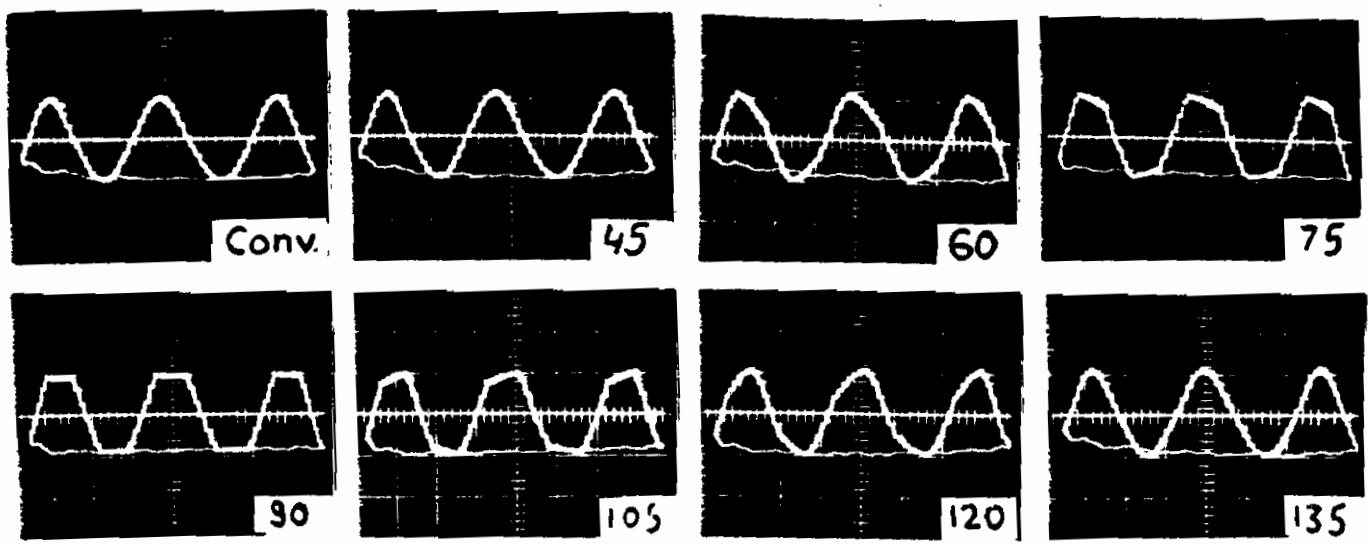

(a) 180° - pole winding spread.

Fig. 4 Resultant M.M.F Oscillographs

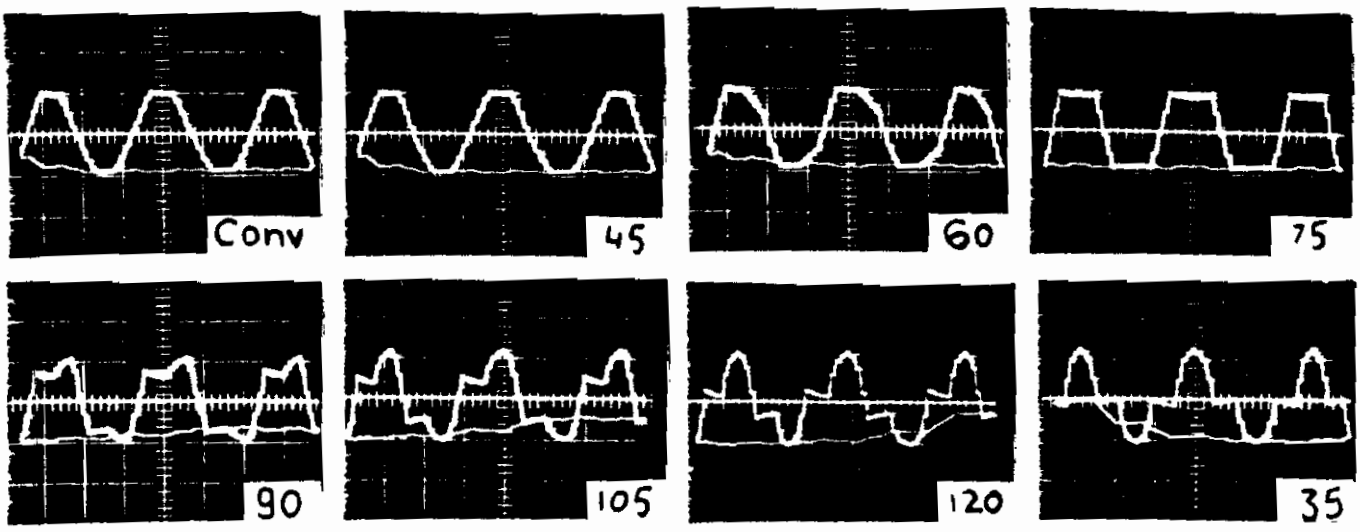

(b) 120° - pole winding spread.

Analytically obtained m.m.f. distributions when the resultant field is shifted in steps w.r.t. the rotor, can be summarised in a representative group of waveforms. Thereby, the effects on the resultant m.m.f. distribution of the shift-angle and of the pole-winding-spread have been studied.

Shifting the resultant field from the d-axis towards the q-axis results in considerable distrotion in the m.m.f. waveform, specially, for shift-angles in the q-axis region and for $\tau \angle 180°$. In addition to the variation in shape and absolute maximum value the distortion extends to include the half-wave duration. This duration becomes equal to the corresponding pole-winding-spread when the resultant field coincides with the q-axis.

The results also show that the analytically obtained waveforms are in good agreement with those obtained from the machine model.

An essential condition to simulate the conventional field distribution by a divided-winding-rotor is that, the resultant field must be directed towards the direct-axis (pole-axis).

7. REFERENCES:

1. ABOU-TABL, H.A.: "Divided-Winding-Rotor Synchronous Generator, No-Load Field Control Factors", Bulletin of the Faculty of Engineering, El-Mansoura University, Vol.III. No. 2 December, 1978.

2. FITZGERALD, A.E., KINGSLEY, C.:"Electric Machinary", Second Edition New York Mc Graw-Hill Book Co., 1961.

3. JAIN, G.C.: "Design, Operation and Testing of Synchronous Machines", Asia Puplishing House Book Co.,1966.

4. COTTON, H.:"Advanced Electrical Technology", Pitman and Sons Ltd, London, 1967.

5. ADKINS, B.: "The General Theory of Electrical Machines", Third Printing, Chapman & Hall Ltd, London, 1962.